**Supplemental Data**

**The 17-residue-long N terminus in huntingtin controls step-wise aggregation in solution and on membranes via different mechanisms**

**Figure S1**

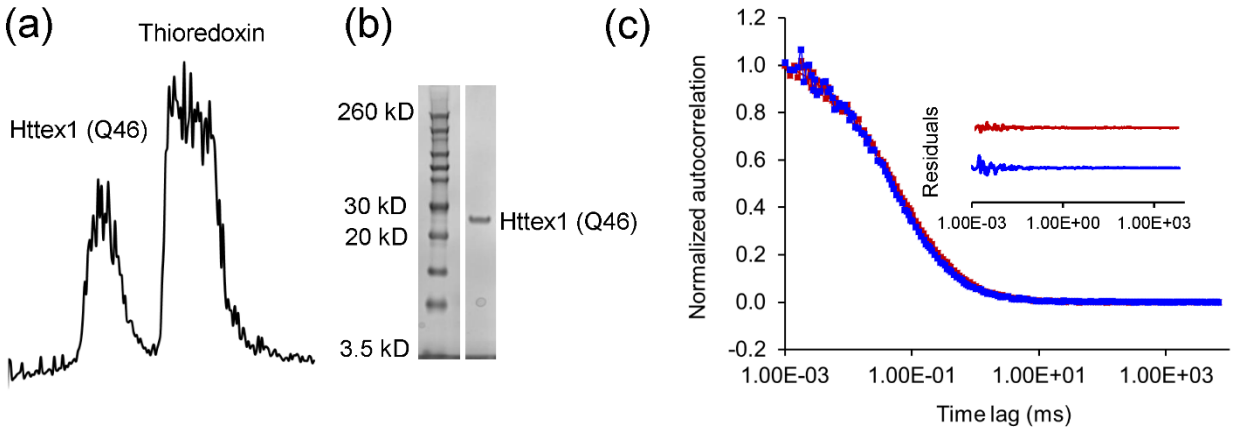


**Figure S1.** (a) Chromatogram for Httex1 purification using a Phenomenex C4 column after enzymatic cleavage of the thioredoxin-Httex1 fusion protein. The identity of the two separate peaks (Httex1 and thioredoxin) was verified by mass spectrometry. (b) SDS-PAGE of purified Httex1 (right lane) shows that the protein runs as a single band at an apparent size comparable to that previously reported (1), left lane is Novex sharp protein standard (3.5 kD-260 kD). Both lanes (left and right) have been spliced from the same gel and are shown together for better clarity (c) FCS autocorrelation data for freshly prepared Httex1(Q46) at 15 µM (red) and Httex1 monomers at highly dilute and sub-saturating concentrations of 10 nM (blue) (2). The close correspondence between the two traces indicates monomeric structures in both cases. The residuals for both fits are shown in the inset of the panel.

**Figure S2**

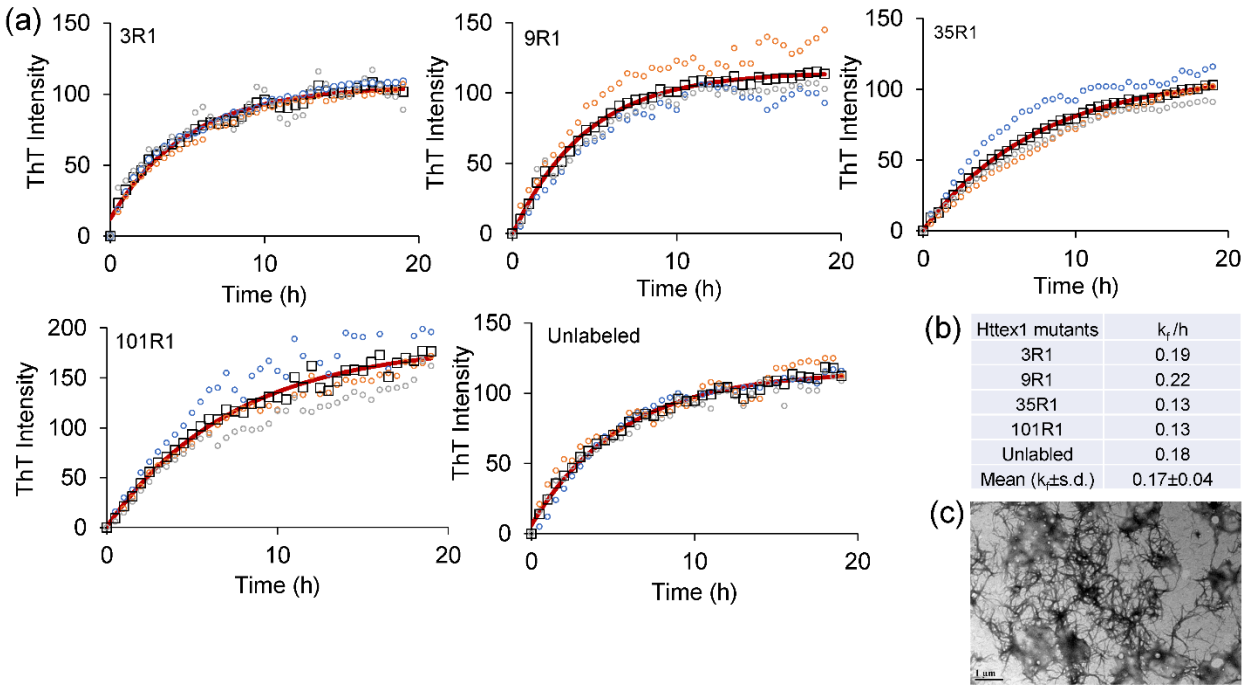


**Figure S2.** (a) The aggregation kinetics for R1-labeled derivatives of Httex1(Q46) (3R1, 9R1, 35R1 and 101R1) and unlabeled (cys-free) Httex1(Q46) were determined by ThT fluorescence under the same conditions that were used in the EPR experiments. Each graph shows three individual measurements (open circles) as well as their mean (open black square). The solid red line represents the fit for the mean data using a single exponential function. (b) The list of time constants ($k_f$) values obtained from the fits shown in (a). (c) A representative TEM image of the 35R1 Httex1(Q46) derivative after 24 h illustrates extensive fibril formation, which was seen for all derivatives.

**Figure S3**

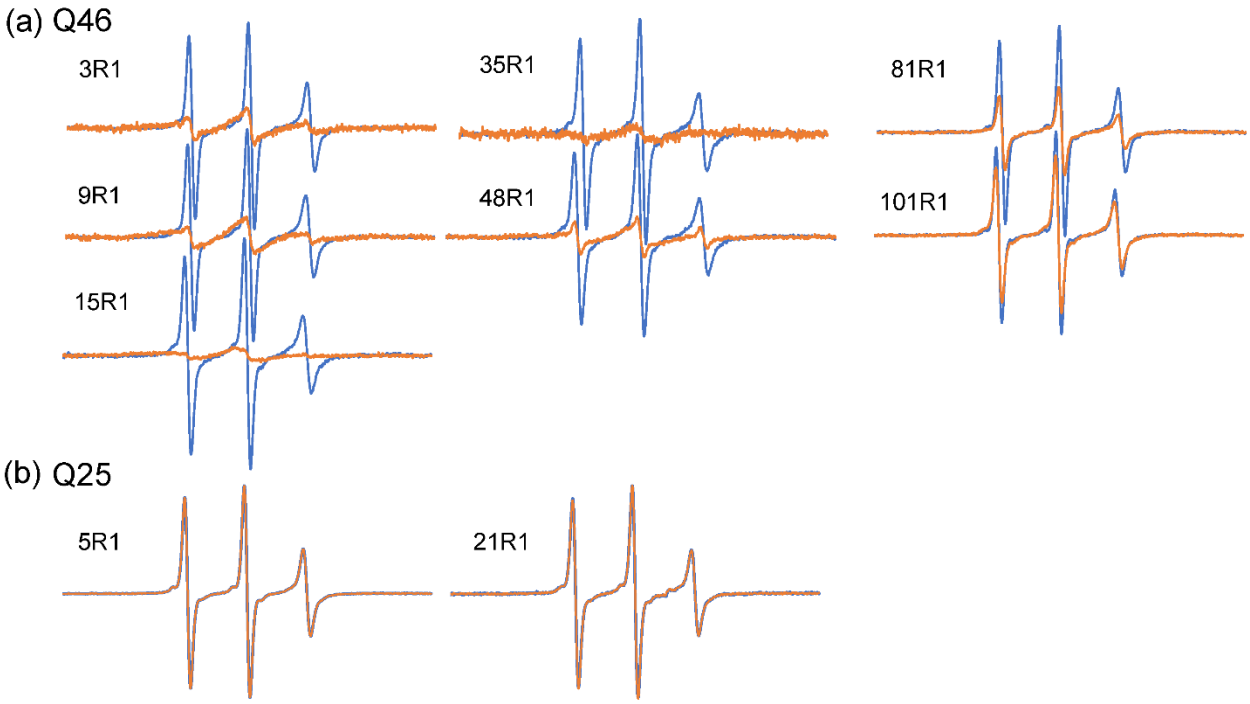


**Figure S3.** The EPR spectra of spin label derivatives of Httex1 are shown in blue at t=0 min and in orange at t=20 h. (a) The representative EPR spectra of Q46 derivatives shows the structural changes occurring in different regions (N17, polyQ and PRD) during misfolding from a highly dynamic structure to a less dynamic structure after fibril formation (b) The EPR spectra of Q25 derivatives 5R1 (N17) and 21R1 (polyQ). There are no changes in the respective EPR spectra over time, suggesting that Httex1(Q25) does not undergo conformational changes and aggregation during the 20-hour time window.

**Figure S4**

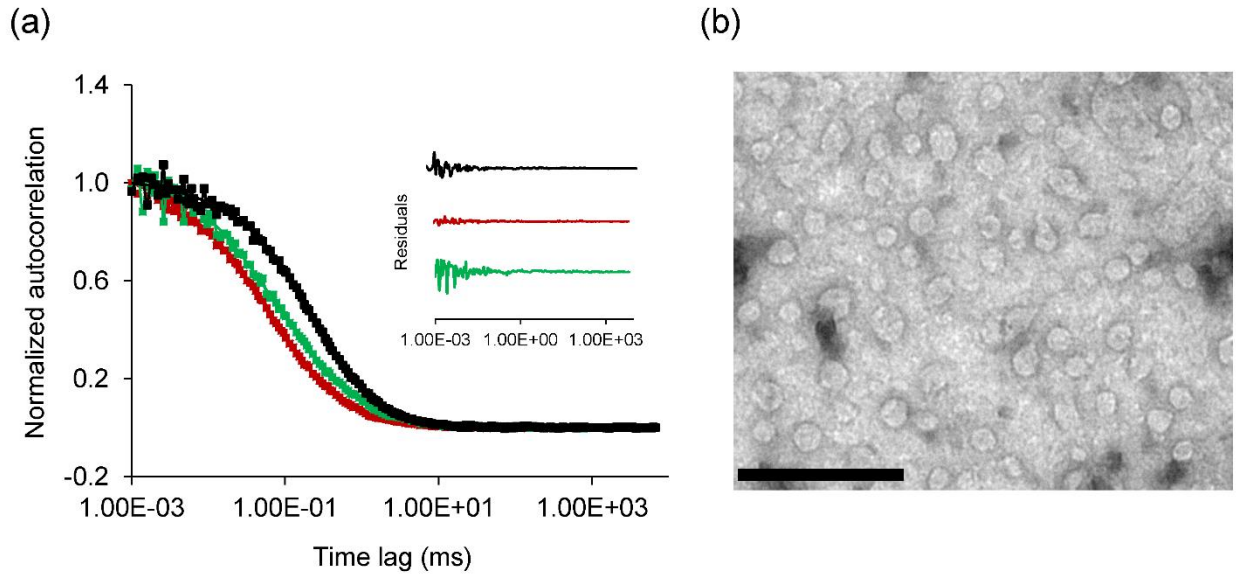


**Figure S4.** (a) FCS autocorrelation of Httex1(Q46). The red curve is for monomeric Httex1 at t= 0 min. The green and black curves depict t=1 h and t=2 h time points, respectively). The residuals (difference between experimental data points and the fits (smooth lines)) are shown as inset in the panel and shown using the same color code. The progressive shift to slower correlation times upon sample maturation over 2 hours is caused by increasing amounts of an oligomeric species with a $\tau_D$ of 220-260 µs. Based on the correlation time for monomer (115 µs), the estimated size of the oligomers is 7-11 subunits. (b) Negatively stained EM images of Httex1(Q46) after 2 hours show predominantly rounded structures with an average diameter of 6.7 nm (1.1 nm standard deviation), likely corresponding to spherical oligomers. The scale bar is 50 nm.

**Figure S5**

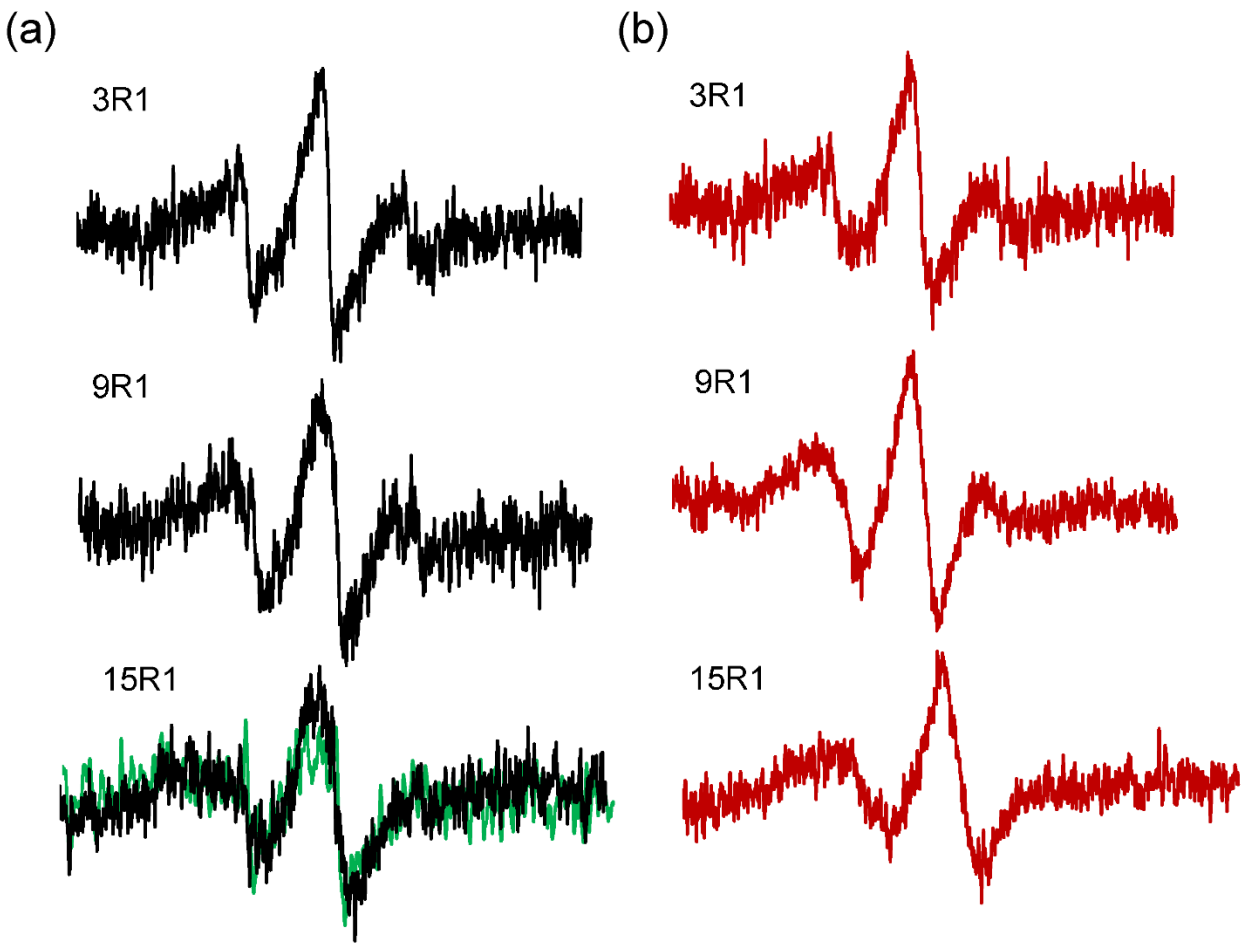


**Figure S5.** (a). The EPR spectra of the early intermediates for labeling sites in the N17 (3R1, 9R1 and 15R1) were obtained from difference spectra of the t=0 min and t=2 h time points. After smoothing, it was possible to also compare the difference spectrum for 15R1 after 30 min (green trace) to that after 2 h (black trace). These curves were very similar in nature indicating similar structural features. (b)**.** The corresponding EPR difference spectra from the final, mostly fibril-containing time points at t=20 h. The overall spectral features for the spectra of a given derivative in (a) and in (b) are very similar, indicating that the early structural features in the N17 largely remain intact until fibril formation.

**Figure S6**

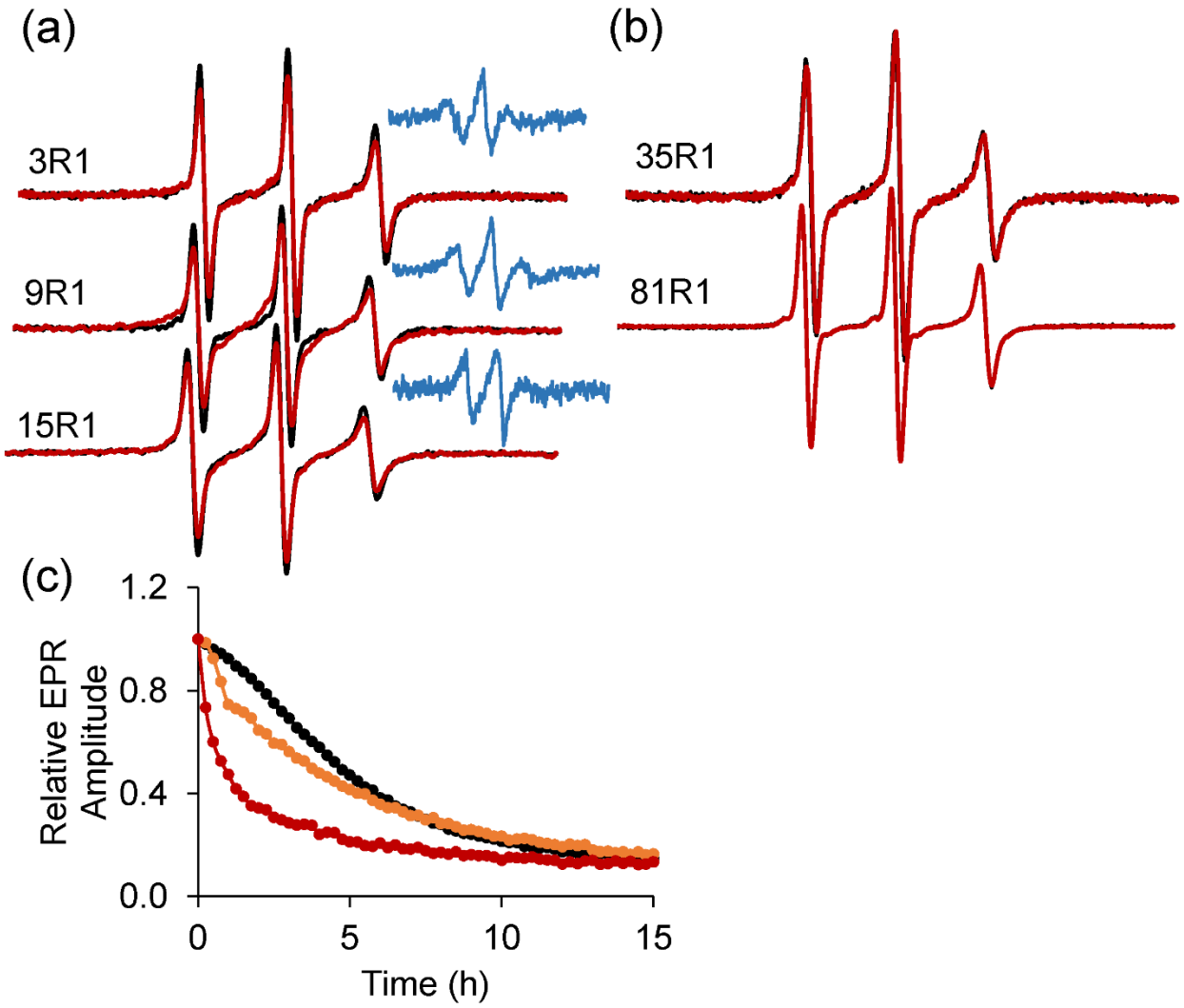


**Figure S6.** The EPR spectra in the absence (black) and presence (red) of membranes with 25% POPS/75% POPC at t=0 min for (a) sites in the N17 (3R1 (top), 9R1 (middle), and 15R1 (bottom)), and (b) sited in the polyQ (35R1 (top)), and PRD (81R1 (bottom). Detectable spectral changes with a drop in signal amplitude are present for all labeling sites in (a) but not (b). The spectra for the lipid-bound state were obtained from the difference of the red and black spectra in (a) and are shown as insets (smaller blue spectra) in the same panel. (c) EPR kinetic data obtained in the presence of 10% POPS/90%POPC and 25% POPS/75% POPC vesicles (375 μM) are shown in orange and red, respectively. The control without membrane is shown in black.

**Figure S7**

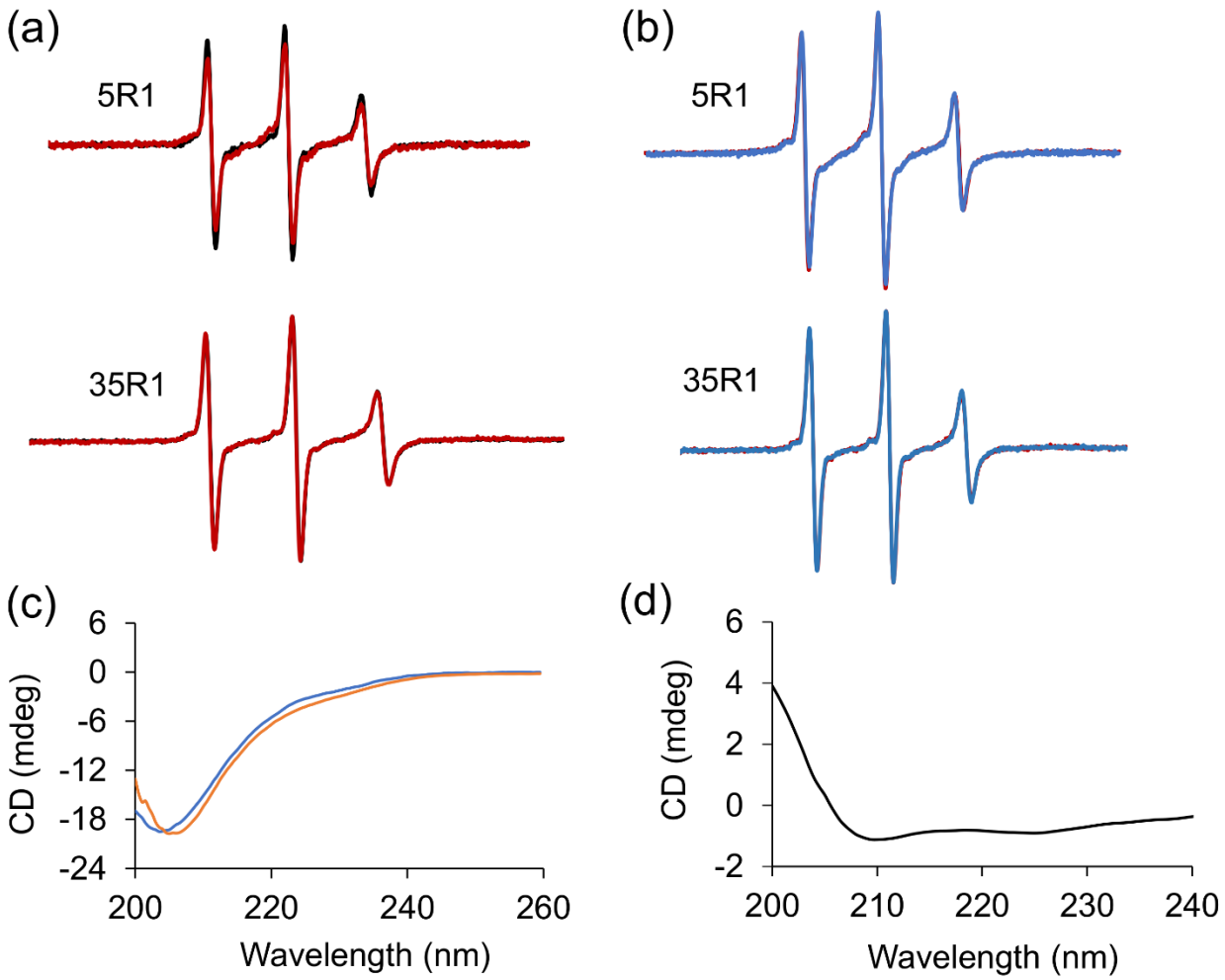


**Figure S7.** (a) An overlay of the EPR spectra of N17 (5R1, top) and polyQ (35R1, bottom) labeled derivatives obtained in the presence (red) and absence (black) of vesicles (25% POPS/75% POPC). A small, but detectable initial drop in amplitude can be seen for 5R1, but not for 35R1. As described in the text, this is interpreted as membrane anchoring by the N17. (b) The EPR spectra for both derivatives do not show any noticeable changes over time, as illustrated with the overlay of the spectra for t=0 min (red) and t=20 h (blue). This result indicates the rapid formation of membrane-anchored structures for Httex1(Q25) that, unlike those for the Q46 derivatives, stay stable over a period of at least 20 h. (c) CD spectra of Httex1(Q25) in the absence (blue) and presence (orange) of vesicles with 25% POPS/75% POPC. (d) The difference spectrum obtained from the spectra in panel (c) shows α-helical character, indicative of increased α-helical structure upon membrane interaction.

**Figure S8**

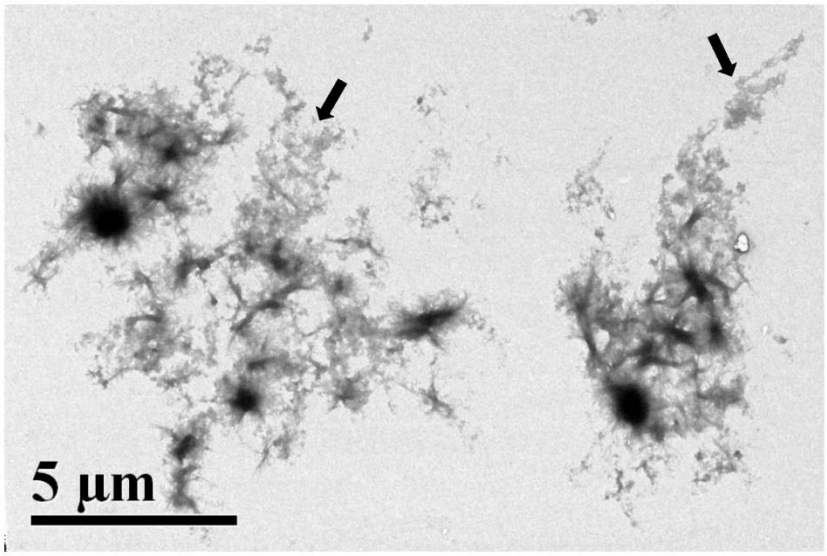


**Figure S8.** The EM image of Httex1 (35R1) obtained 3 hours after addition of vesicles (25% POPS/75% POPC) show bundles and clusters of fibrils. Notably absent in all images were vesicles. The black arrows point to amorphous structures that may contain membrane debris.

## References

1. Vieweg, S.; Ansaloni, A.; Wang, Z. M.; Warner, J. B.; Lashuel, H. A., *J Biol Chem* **2016,** *291* (23), 12074-86.

2. Crick, S. L.; Jayaraman, M.; Frieden, C.; Wetzel, R.; Pappu, R. V., *Proc Natl Acad Sci U S A* **2006,** *103* (45), 16764-9.